


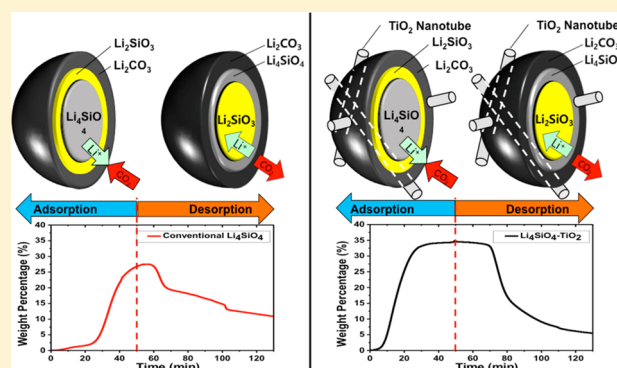
Enhanced Sorption Cycle Stability and Kinetics of CO₂ on Lithium Silicates Using the Lithium Ion Channeling Effect of TiO₂ Nanotubes

Joo Sung Lee and Cafer T. Yavuz*

Graduate school of Energy, Environment, Water and Sustainability (EEWS), Korea Advanced Institute of Science and Technology (KAIST), Daejeon, 34141, Republic of Korea

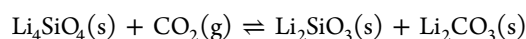
Supporting Information

ABSTRACT: Lithium silicate (Li₄SiO₄) is a promising high temperature CO₂ sorbent because of its large CO₂ capacity at elevated temperatures with low materials cost. However, the conventional nonporous Li₄SiO₄ shows very poor CO₂ adsorption kinetics. Thus, a Li₄SiO₄–TiO₂ nanotubes complex was synthesized where LiOH and fumed silica would be calcined around TiO₂ nanotubes. TiO₂ nanotubes in Li₄SiO₄ structure functioning as open highways, lithium ions were able to channel through the bulky structure and enhance the sorption kinetics, leading the total adsorption capacity to near theoretical values. Furthermore, cyclic studies at 700 °C revealed strong stability over at least 10 cycles. These findings indicate that stability and kinetics of CO₂ sorption can be greatly improved by the nanotube composites of known adsorbents.



1. INTRODUCTION

Strong economic dependency on the use of fossil fuels as a main source of affordable energy has led to a growing concern of increasing CO₂ emission rates.^{1–6} The majority of global CO₂ emission occurs from fossil fuel powered plants, and the CO₂ emission rate can significantly be reduced if an effective CO₂ absorbent is used at the flue gas stream.³ Moreover, some promising studies are focused on retrofitting CO₂ absorbents to a steam methane reformer (SMR).^{7–12} The SMR operates at high temperatures (700–1100 °C),¹² converting methane gas in steam to form H₂ gas and CO₂ gas as a product. With an appropriate CO₂ absorbent that effectively captures CO₂ at the operating temperature of the SMR in the system, the H₂ production rate can be further enhanced. Among the several CO₂ absorbents that operate at high temperature regions, there are several known lithium-based solid metal oxides such as lithium zirconate,¹³ lithium aluminate,¹⁴ and lithium silicate.^{15–27} Lithium silicate (Li₄SiO₄) is one of the favorable candidates²³ with low cost materials, easy synthesis, high regenerability,¹⁹ and has an outstanding theoretical capacity of 36.7 wt %.¹⁹ The chemisorption reaction proceeds as follows:



However, as the chemisorption reaction proceeds (Figure 1), the Li₂SiO₃ and Li₂CO₃ layer forms on the surface of the structure.¹⁹ As Li₄SiO₄ has a very low surface area (~1 m²/g),²⁶ lithium silicate suffers from slow kinetics in CO₂ sorption as it reaches theoretical uptake capacity due to the interference in lithium ion transfer.

TiO₂ nanotubes offer a resilient channel-forming component when heterogeneously introduced to the inorganic media.

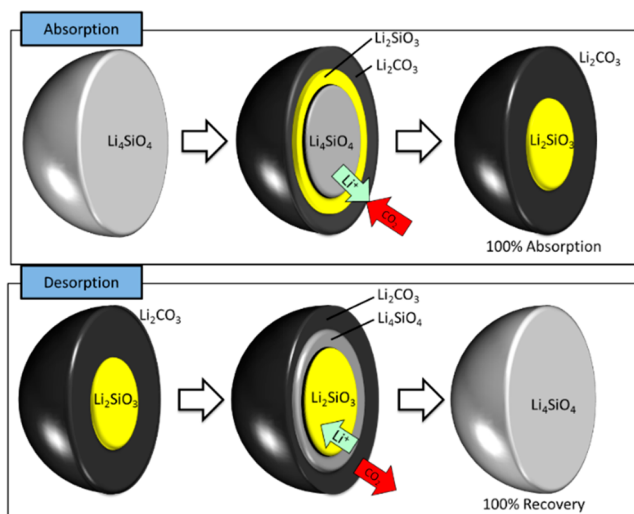


Figure 1. Schematic representation of an ideal CO₂ sorption mechanism of conventional Li₄SiO₄. The sorption cycle is not practical due to the slow kinetics.

There are several fine examples that exist in the literature where TiO₂ nanotubes contribute an open channel structure to promote channeling gas flow and reduce diffusion limitation.^{28–30} For example, TiO₂ nanotubes were used to enhance

Received: December 20, 2016

Revised: February 20, 2017

Accepted: March 2, 2017

Published: March 2, 2017



lithium ion diffusion for ultrafast rechargeable lithium ion batteries.³¹

This study intends to impregnate TiO₂ nanotubes in the conventional Li₄SiO₄ structures in order to create channels for lithium ion transfer during CO₂ adsorption desorption cycles.^{20,32} With channeling enhanced lithium ion transfer throughout the overall structure, we observed not only an increase in the overall surface area of the nonporous nature of the lithium silicate but also significantly enhanced kinetics of CO₂ sorption.

2. EXPERIMENTAL SECTION

2.1. Materials and Reagents. P25 titanium dioxide, fumed silica, and nitric acid were obtained from Sigma-Aldrich, while the sodium hydroxide and lithium hydroxide were obtained from Samchun Chemicals. All chemicals were used as is, unless otherwise stated. For extended experimental details see Materials and Methods in the [Supporting Information](#).

2.2. Synthesis of TiO₂ Nanotube and Impregnation in Li₄SiO₄. TiO₂ nanotube was synthesized using 0.1 g of P25 TiO₂ added to a 10 M NaOH solution and dispersed for 5 min. The mixture was then transferred to an autoclave with a magnetic stirrer, and placed in a silicon oil-bath at 130 °C for 24 h under continuous stirring at 200 rpm. Once the reaction was completed, the product was removed and washed with deionized water until a pH level of 9 was reached. To neutralize and replenish the surface protons, 0.1 M HNO₃ solution was used to wash the product three times. It was then washed with deionized water to neutralize the pH to 7. The TiO₂ nanotube sludge was dried for 12 h.³¹ To synthesize the Li₄SiO₄–TiO₂ nanotube structure, 4.1:1 molar ratio of LiOH and fumed silica were mixed with TiO₂ nanotubes in 9:1 weight ratio and thermally treated in an alumina crucible at 700 °C under N₂ to obtain the Li₄SiO₄–TiO₂ nanotube complex.

2.3. Material Characterization. To analyze surface area and morphology, specific surface areas are determined by N₂ adsorption (Micrometrics Triflex) using the Brunauer–Emmett–Teller (BET) method at 77 K with the sample degassed at 400 °C for 8 h in dry He flow. Pore size was calculated using the DFT pore size distribution calculation with 2D-NLDFT, N₂ carbon finite AS = 6 model. Surface textural properties and morphologies were analyzed using field emission scanning electron microscope (SEM, Magellan 400) with light osmium coating to reduce the charge on the images. Structural analysis was performed on D/MAX-2500 (Rigaku) for powder X-ray diffraction patterns equipped with Cu K α radiation (40 kV, 450 mA). Scattering patterns were acquired from 5° to 70° with increments of 0.01°. For gravimetric analysis, adsorption and desorption measurements were collected using DTG-60 (Shimadzu). Initially, the temperature was raised to 700 °C at a ramping rate of 20 °C/min and held for 10 min for stabilization using N₂ gas. For adsorption, the N₂ gas was switched to CO₂ gas for 70 min, and for desorption the gas was switched back to N₂ for 60 min then raised to 720 °C for further desorption. The flow rate of N₂ gas and CO₂ gas were kept consistent at 50 mL/min throughout the experiment. CO₂ adsorption and desorption cyclic analysis was performed by first raising the temperature to 700 °C at a ramping rate of 20 °C/min and holding for 10 min for stabilization under N₂ gas. For adsorption, inlet gas was switched to CO₂ for 70 min where mass increase reached equilibrium. For desorption, feed gas was switched back to N₂ for 60 min. Adsorption and desorption events were alternated 10 times for cyclic analysis.

3. RESULTS AND DISCUSSION

The obtained composites allowed us to study CO₂ kinetics as well as to find ways in improving uptake capacity to theoretical uptake value. By impregnating TiO₂ nanotubes in Li₄SiO₄ structure, nanotubes are expected to function as a lithium ion channel to enhance chemisorption. To identify its surface morphology subsequent to the effects of TiO₂ nanotube impregnation, field emission SEM was used ([Figure 2](#)).

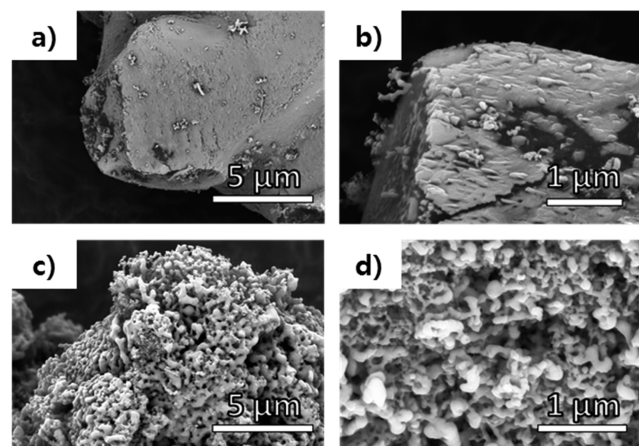


Figure 2. SEM images of (a,b) bulk Li₄SiO₄ after 700 °C formation through calcination, (c,d) Li₄SiO₄–TiO₂ nanotube complex after 700 °C formation through calcination.

Note that, due to charging on the surface of lithium silicate even with osmium coating, the back scattered electron detector mode (BSE mode) was used to get a clearer image of the surfaces of both lithium silicate and lithium silicate–TiO₂ nanotube.

Bulk lithium silicate ([Figure 2a,b](#)) possesses a hard-edged nonporous structure. On the other hand, when the TiO₂ nanotube was added to lithium silicate ([Figure 2c,d](#)), lithium silicate has formed surrounding the TiO₂ nanotube. It was identified that with TiO₂ nanotube impregnation in forming lithium silicate, the overall structure morphology tended to be more rough indicating inherent porosity (see corresponding elemental maps for Li₄SiO₄ and Li₄SiO₄–TiO₂ nanotube and SEM image of TiO₂ nanotube in the [Supporting Information](#), SI).

The results obtained for surface area by BET method are summarized in [Table 1](#) (see corresponding gas adsorption

Table 1. Texture Analysis of Lithium Silicate Structures Used in This Work^a

	SA _{BET} (m ² /g)	pore volume (cm ³ /g)	pore size (Å)
conventional Li ₄ SiO ₄ , 700 °C	1.1	N/A	N/A
Li ₄ SiO ₄ –TiO ₂ NT, 700 °C	4.0	N/A	N/A
TiO ₂ NT	35.7	0.144	147.8

^aSA_{BET}, surface area from Brunauer–Emmett–Teller; NT, nanotube.

isotherms in the [Supporting Information](#)). As expected, the pure lithium silicate does not have any porosity. On the other hand, with TiO₂ nanotube impregnation, surface area of lithium silicate has increased. Calculating the fact that 10% of TiO₂ nanotube was impregnated in Li₄SiO₄–TiO₂ nanotube structure, surface area of the composite is around what was expected.

To identify the state of $\text{Li}_4\text{SiO}_4\text{-TiO}_2$ structure after the heat treatment at 700 °C, XRD diffraction patterns were analyzed (Figure 3).

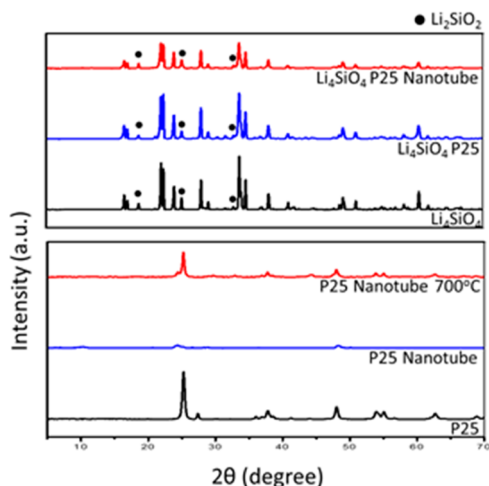


Figure 3. XRD patterns of Li_4SiO_4 complex and various P25 TiO_2 forms.

When P25 is elongated to form a nanotube, it loses its crystallinity and becomes amorphous (Figure 3). However, when the nanotube is heated to 700 °C, new peaks start to appear. In the case when TiO_2 nanotube is impregnated to Li_4SiO_4 structure, since the TiO_2 percentage in overall structure is too low to be identified in XRD, the corresponding peaks are not distinguishable.

The new $\text{Li}_4\text{SiO}_4\text{-TiO}_2$ composites were tested in TGA for their CO_2 absorption (see Figure 4 below and Figure S7

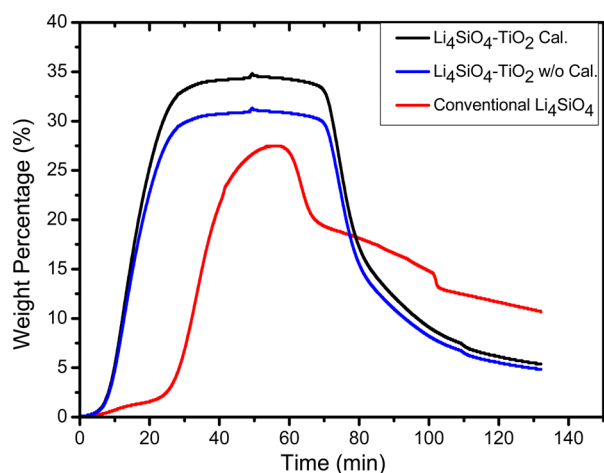


Figure 4. TGA curve of lithium silicates with and without TiO_2 nanotube impregnation. “Cal.” indicates calculation that has been conducted in order to exclude TiO_2 nanotube from the absorption data, as TiO_2 nanotubes are known not to interact with CO_2 at these temperatures.

in Supporting Information). As Li_4SiO_4 is known to capture CO_2 near 700 °C, the temperature was increased to 700 °C with N_2 conditions and then switched to CO_2 to measure the weight difference.

Li_4SiO_4 that had a TiO_2 nanotube implant has shown a significant increase in CO_2 capacity as compared to Li_4SiO_4 due

to its availability of active sites, thus resulting in more drastic increases in CO_2 sorption kinetics. For more direct comparison on Li_4SiO_4 itself, as the 10% of TiO_2 does not interact with the CO_2 , the amount of TiO_2 has been excluded from the overall weight percentage using the formula below (see CO_2 absorption of TiO_2 nanotube in transient TGA analysis in Supporting Information):

$$\text{calculated wt\%} = \frac{\text{chemisorbed mass of } \text{Li}_4\text{SiO}_4 \cdot \text{TiO}_2 \text{ composite} - \text{mass of } \text{TiO}_2}{\text{original mass of } \text{Li}_4\text{SiO}_4 \cdot \text{TiO}_2 \text{ composite} - \text{mass of } \text{TiO}_2}$$

The calculated values give more reliable uptake capacity and kinetics. A total CO_2 uptake increase of 34.5 wt % comes close to the theoretical maximum uptake of CO_2 in Li_4SiO_4 , 36.7 wt %. Additionally, the $\text{Li}_4\text{SiO}_4\text{-TiO}_2$ structure has shown significantly faster sorption rates as well. Note that pure Li_4SiO_4 responds slower as compared to a $\text{Li}_4\text{SiO}_4\text{-TiO}_2$ structure, proving $\text{Li}_4\text{SiO}_4\text{-TiO}_2$ can start absorbing at lower concentrations of CO_2 .

A cyclic CO_2 absorption and desorption experiment on $\text{Li}_4\text{SiO}_4\text{-TiO}_2$ nanotube composite was carried out at 700 °C using pure CO_2 for absorption and pure N_2 for desorption (Figure 5). After the first absorption and desorption cycle, the

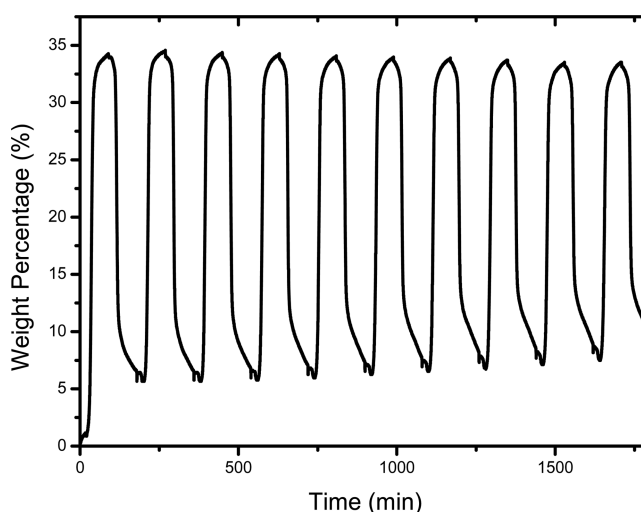


Figure 5. TGA curve of the cyclic study using $\text{Li}_4\text{SiO}_4\text{-TiO}_2$ nanotube composite (10 cycles at 700 °C with CO_2 for absorption and N_2 for desorption).

uptake capacity has slightly increased due to the opening of more surface area in the inner structure of Li_4SiO_4 , and maintains it without any decrease in either absorption or desorption capacity or kinetics with working absorption and desorption capacity of 28%. The result thus concludes that the $\text{Li}_4\text{SiO}_4\text{-TiO}_2$ nanotube withstands the temperature of 700 °C without any sintering, but undergoes slight reorientation in the early stages of the absorption and desorption cycles to provide openings for more active sites, which further improves its uptake capacity as well as its kinetics.

Even after 10 cycles of CO_2 adsorption and desorption cycles, surface morphology has not been significantly deformed as compared to its initial morphology, proving its strong stability in the operating temperatures (Figure 6). We have also studied FTIR analysis of the sorbents before and after cycles and found that the structural integrity is preserved (see Figure S10 in Supporting Information).

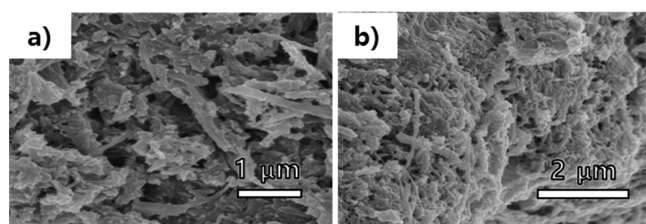


Figure 6. SEM images of $\text{Li}_4\text{SiO}_4\text{-TiO}_2$ nanotubes after 10 cycles of CO_2 sorption.

4. CONCLUSIONS

In the present work, we have synthesized Li_4SiO_4 with TiO_2 nanotubes using a simple solid-state formation method. Synthesis initially required P25 TiO_2 that has been elongated to form a nanotube, which is then combined with LiOH and fumed silica for the synthesis of the $\text{Li}_4\text{SiO}_4\text{-TiO}_2$ nanotube complex. Although XRD analysis does not show significant TiO_2 dosage in the curve, a SEM image clearly shows TiO_2 nanotube implants within the structure of Li_4SiO_4 . We suspect that through TiO_2 nanotubes acting as channels for lithium ions to move freely within the bulky structure of conventional Li_4SiO_4 , a significant increase in the kinetics of CO_2 absorption and desorption were identified. Furthermore, with the strong channeling effects of TiO_2 nanotubes, lithium ions that were not able to diffuse to the active sites in a conventional Li_4SiO_4 were able to reach to the active surface area and capture CO_2 , thus increasing the CO_2 absorption capacity to near the theoretical maximum capacity value. The absorption and desorption cycles at 700°C were studied for 10 cycles and have shown strong stability under high temperatures without a significant decrease in the absorption capacity or the kinetics. The present method provides a simple synthesis of a $\text{Li}_4\text{SiO}_4\text{-TiO}_2$ structure with significantly improved performance in CO_2 absorption applications relative to the conventional Li_4SiO_4 . This improved $\text{Li}_4\text{SiO}_4\text{-TiO}_2$ structure could be a strong candidate for many CO_2 sequestration applications.

■ ASSOCIATED CONTENT

Supporting Information

The Supporting Information is available free of charge on the ACS Publications website at DOI: 10.1021/acs.iecr.6b04918.

Materials and Methods, and SEM, EDS, TGA, and BET analyses (PDF)

■ AUTHOR INFORMATION

Corresponding Author

*E-mail: yavuz@kaist.ac.kr. Tel: (+82) 42 350 1718.

ORCID

Cafer T. Yavuz: 0000-0003-0580-3331

Notes

The authors declare no competing financial interest.

■ ACKNOWLEDGMENTS

We acknowledge the financial support by the National Research Foundation of Korea (NRF) grant funded by the Korea government (MSIP) (No. NRF-2016R1A2B4011027).

■ REFERENCES

(1) Zulfikar, S.; Sarwar, M. I.; Yavuz, C. T. Melamine Based Porous Organic Amide Polymers for CO_2 Capture. *RSC Adv.* **2014**, *4* (94), 52263–52269.

(2) Zulfikar, S.; Awan, S.; Karadas, F.; Atilhan, M.; Yavuz, C. T.; Sarwar, M. I. Amidoxime Porous Polymers for CO_2 Capture. *RSC Adv.* **2013**, *3* (38), 17203–17213.

(3) D'Alessandro, D. M.; Smit, B.; Long, J. R. Carbon Dioxide Capture: Prospects for New Materials. *Angew. Chem., Int. Ed.* **2010**, *49* (35), 6058–6082.

(4) Wang, C.; Dou, B.; Song, Y.; Chen, H.; Xu, Y.; Xie, B. High Temperature CO_2 Sorption on Li_2ZrO_3 Based Sorbents. *Ind. Eng. Chem. Res.* **2014**, *53* (32), 12744–12752.

(5) Wang, Q.; Luo, J.; Zhong, Z.; Borgna, A. CO_2 Capture by Solid Adsorbents and Their Applications: Current Status and New Trends. *Energy Environ. Sci.* **2011**, *4* (1), 42–55.

(6) Ullah, R.; Atilhan, M.; Anaya, B.; Al-Muhtaseb, S.; Aparicio, S.; Thirion, D.; Yavuz, C. T. High Performance CO_2 Filtration and Sequestration by Using Bromomethyl Benzene Linked Microporous Networks. *RSC Adv.* **2016**, *6* (70), 66324–66335.

(7) Gil, M. V.; Feroso, J.; Rubiera, F.; Chen, D. H_2 Production by Sorption Enhanced Steam Reforming of Biomass-derived Bio-oil in a Fluidized Bed Reactor: An Assessment of the Effect of Operation Variables Using Response Surface Methodology. *Catal. Today* **2015**, *242* (Part A), 19–34.

(8) Hou, K.; Hughes, R. The kinetics of methane steam reforming over a $\text{Ni}/\alpha\text{-Al}_2\text{O}_3$ catalyst. *Chem. Eng. J.* **2001**, *82* (1–3), 311–328.

(9) Hufton, J. R.; Mayorga, S.; Sircar, S. Sorption-enhanced reaction process for hydrogen production. *AIChE J.* **1999**, *45* (2), 248–256.

(10) Rostrup-Nielsen, J. R. Catalytic Steam Reforming. In *Catalysis: Science and Technology*; Anderson, J. R., Boudart, M., Eds.; Springer: Berlin, Heidelberg, 1984; pp 1–117.

(11) Xu, J.; Froment, G. F. Methane steam reforming, methanation and water-gas shift: I. Intrinsic kinetics. *AIChE J.* **1989**, *35* (1), 88–96.

(12) Iliuta, I.; Radfarnia, H. R.; Iliuta, M. C. Hydrogen Production by Sorption-Enhanced Steam Glycerol Reforming: Sorption Kinetics and Reactor Simulation. *AIChE J.* **2013**, *59* (6), 2105–2118.

(13) Ida, J.-i.; Lin, Y. S. Mechanism of High-Temperature CO_2 Sorption on Lithium Zirconate. *Environ. Sci. Technol.* **2003**, *37* (9), 1999–2004.

(14) Ávalos-Rendón, T.; Casa-Madrid, J.; Pfeiffer, H. Thermochemical Capture of Carbon Dioxide on Lithium Aluminates (LiAlO_2 and Li_5AlO_4): A New Option for the CO_2 Absorption. *J. Phys. Chem. A* **2009**, *113* (25), 6919–6923.

(15) Duan, Y.; Luebke, D.; Pennline, H. H. Efficient Theoretical Screening of Solid Sorbents for CO_2 Capture Applications. *Int. J. Clean Coal Energy* **2012**, *1* (1), 1–11.

(16) Duan, Y.; Pfeiffer, H.; Li, B.; Romero-Ibarra, I. C.; Sorescu, D. C.; Luebke, D. R.; Halley, J. W. CO_2 capture properties of lithium silicates with different ratios of $\text{Li}_2\text{O}/\text{SiO}_2$: an ab initio thermodynamic and experimental approach. *Phys. Chem. Chem. Phys.* **2013**, *15* (32), 13538–13558.

(17) Harrison, D. P. Sorption-Enhanced Hydrogen Production: A Review. *Ind. Eng. Chem. Res.* **2008**, *47* (17), 6486–6501.

(18) Kato, M.; Yoshikawa, S.; Nakagawa, K. Carbon dioxide absorption by lithium orthosilicate in a wide range of temperature and carbon dioxide concentrations. *J. Mater. Sci. Lett.* **2002**, *21* (6), 485–487.

(19) Kim, H.; Jang, H. D.; Choi, M. Facile synthesis of macroporous Li_4SiO_4 with remarkably enhanced CO_2 adsorption kinetics. *Chem. Eng. J.* **2015**, *280*, 132–137.

(20) Nair, B. N.; Burwood, R. P.; Goh, V. J.; Nakagawa, K.; Yamaguchi, T. Lithium based ceramic materials and membranes for high temperature CO_2 separation. *Prog. Mater. Sci.* **2009**, *54* (5), 511–541.

(21) Olivares-Marín, M.; Drage, T. C.; Maroto-Valer, M. M. Novel lithium-based sorbents from fly ashes for CO_2 capture at high temperatures. *Int. J. Greenhouse Gas Control* **2010**, *4* (4), 623–629.

(22) Pfeiffer, H.; Bosch, P.; Bulbulian, S. Synthesis of lithium silicates. *J. Nucl. Mater.* **1998**, *257* (3), 309–317.

(23) Rodríguez-Mosqueda, R.; Pfeiffer, H. Thermokinetic Analysis of the CO_2 Chemisorption on Li_4SiO_4 by Using Different Gas Flow Rates and Particle Sizes. *J. Phys. Chem. A* **2010**, *114* (13), 4535–4541.

- (24) Shan, S.; Li, S.; Jia, Q.; Jiang, L.; Wang, Y.; Peng, J. Impregnation Precipitation Preparation and Kinetic Analysis of Li_4SiO_4 -Based Sorbents with Fast CO_2 Adsorption Rate. *Ind. Eng. Chem. Res.* **2013**, *52* (21), 6941–6945.
- (25) Subha, P. V.; Nair, B. N.; Hareesh, P.; Mohamed, A. P.; Yamaguchi, T.; Warrier, K. G. K.; Hareesh, U. S. CO_2 Absorption Studies on Mixed Alkali Orthosilicates Containing Rare-Earth Second-Phase Additives. *J. Phys. Chem. C* **2015**, *119* (10), 5319–5326.
- (26) Venegas, M. J.; Fregoso-Israel, E.; Escamilla, R.; Pfeiffer, H. Kinetic and Reaction Mechanism of CO_2 Sorption on Li_4SiO_4 : Study of the Particle Size Effect. *Ind. Eng. Chem. Res.* **2007**, *46* (8), 2407–2412.
- (27) Xiang, M.; Zhang, Y.; Hong, M.; Liu, S.; Zhang, Y.; Liu, H.; Gu, C. CO_2 absorption properties of Ti- and Na-doped porous Li_4SiO_4 prepared by a sol–gel process. *J. Mater. Sci.* **2015**, *50* (13), 4698–4706.
- (28) Roy, P.; Berger, S.; Schmuki, P. TiO_2 Nanotubes: Synthesis and Applications. *Angew. Chem., Int. Ed.* **2011**, *50* (13), 2904–2939.
- (29) Weon, S.; Choi, W. TiO_2 Nanotubes with Open Channels as Deactivation-Resistant Photocatalyst for the Degradation of Volatile Organic Compounds. *Environ. Sci. Technol.* **2016**, *50* (5), 2556–2563.
- (30) Wagemaker, M.; Kentgens, A. P. M.; Mulder, F. M. Equilibrium lithium transport between nanocrystalline phases in intercalated TiO_2 anatase. *Nature* **2002**, *418* (6896), 397–399.
- (31) Tang, Y.; Zhang, Y.; Deng, J.; Wei, J.; Tam, H. L.; Chandran, B. K.; Dong, Z.; Chen, Z.; Chen, X. Mechanical Force-Driven Growth of Elongated Bending TiO_2 -based Nanotubular Materials for Ultrafast Rechargeable Lithium Ion Batteries. *Adv. Mater.* **2014**, *26* (35), 6111–6118.
- (32) Qiu, B.; Xing, M.; Zhang, J. Mesoporous TiO_2 Nanocrystals Grown in Situ on Graphene Aerogels for High Photocatalysis and Lithium-Ion Batteries. *J. Am. Chem. Soc.* **2014**, *136* (16), 5852–5855.